Large Scale Parallel Computing and Scalability Study for Surface Combatant Static Maneuver and Straight Ahead Conditions Using CFDShip-Iowa

F. STERN, S. BHUSHAN, P. CARRICA and J. YANG

ABSTRACT

Scalability studies are performed for CFDShip-Iowa URANS/DES curvilinear and Cartesian grid solvers and calculations are performed using largest grids to date. Verification and validation study is performed for V4-DES solution for DTMB 5415 with bilge keels at 20° static drift using up to 250M grid. The instantaneous and mean flow field is analyzed to identify flow separation patterns, vortical structures and associated instabilities. V6 RANS solution of 5415 bare hull at straight ahead condition on 276M grid is compared with benchmark V4-blended k-ω/k-ε, V4-wall-function, V4-DES results and EFD data to identify limitations of wall-layer modeling using WF for immersed boundary method.

INTRODUCTION

Large scale computations are important for ship flows as they enable resolution of small-scale physics, improve our understanding of turbulent and vortical structures, two phase flows and air entrainment, help in identifying modeling issues and develop better models. Herein, calculations are performed using largest grids to date for CFDShip-Iowa unsteady Reynolds averaged Navier-Stokes (URANS)/ Detached eddy simulation (DES) toolbox solvers which include both curvilinear (V4) and Cartesian grid (V6) solvers. The objective of this paper is to study scalability and identify scalability bottlenecks, and to validate V4 and V6 predictions. The scalabilities of V4 and V6 are studied up to 2300 processors. V4 simulation is performed for surface combatant DTMB 5415 (5415 henceforth) with bilge keels at 20° static drift on 250M grid. The study focuses on analysis of the turbulent and vortical structures, associated instabilities including verification and validation (V&V). V6 simulation is performed for 5415 bare hull at straight ahead condition on a 276M grid using WF with $y^+ = 30$ to identify limitations of wall-layer modeling using wall-function (WF) for immersed

IIHR-Hydroscience and Engineering, The University of Iowa, Iowa City, IA 52242-1585

boundary method (IBM). For this case, V4- blended k-ω/k-ε (BKW), -WF simulations on 615K grid and –DES on 300M grid are also performed to obtain benchmark results.

The general-purpose code V4 solves the URANS/DES equations in the liquid phase of a free-surface flow [1]. The governing equations are solved in absolute inertial earth-fixed or relative inertial coordinates for an arbitrary non-deforming control volume [2]. The turbulence modeling is performed using BKW or anisotropic Reynolds stress (ARS) models and has DES [3] and WF [4] options. The interface modeling is performed using single-phase level-set methods. A multi-block dynamic overset grid approach is used to allow relative motions between the grids for six degrees of freedom (6DoF) ship motions [5]. The overset grid interpolation coefficients are obtained using SUGGAR [6]. The code provides propeller modeling using simplified body-force or direct discretization, and has a proportional-integral-differential (PID) controller to allow self-propulsion or auto-piloted simulations [7]. The governing equations are discretized using cell-centered finite difference schemes on body-fitted curvilinear grids and solved using a predictor-corrector method. The time marching is done using the 2^{nd} order backward difference scheme, the convection terms are discretized using a 2^{nd} or hybrid $2^{nd}/4^{th}$ order upwind or TVD schemes, and 2^{nd} order upwind or TVD schemes are used for level-set [8]. The pressure Poisson equation is solved using the PETSc toolkit and either PISO or projection algorithm is used to satisfy continuity. Message Passing Interface (MPI) based domain decomposition is used, where each decomposed block is mapped to a single processor. The code was modified with the help of software experts at ANL to reduce memory requirements, and optimize the serial and parallel performance of numerical algorithms. A recent set of large scale computations on AFRL SGI Altix 4700 (Hawk) using 60-115M grids on 276-500 processors includes forward speed diffraction and pitch and heave problems for 5415 for Fr = 0.28 and 0.41, respectively [9].

In V6 the URANS/DES/ Large eddy simulation (LES) two-phase flow governing equations are solved in absolute inertial earth-fixed coordinates using IBM [10]. The turbulence modeling is performed using either BKW or k-g/k-ε (BKG) models with WF for URANS or a dynamic Smagorinsky model for LES. The interface modeling is performed using level-set, particle level-set [11] or coupled level-set and volume-of-fluid (CLSVOF) method [12]. The governing equations are discretized using finite differences on a non-uniform staggered Cartesian grid and solved using a four-step fractional-step method [10,13]. The time marching is performed using a semi-implicit second-order scheme, the convection terms are discretized using 3^{rd} order QUICK/5^{th} order WENO schemes, and level-set equation are solved using 3^{rd} order TVD/5^{th} order WENO schemes. The pressure Poisson equation is solved using the Krylov subspace based multi-grid PETSc library or the semi-coarsening multi-grid HYPRE library. The code uses MPI based domain decomposition for solution on parallel processors and MPI-I/O. The code has not yet undergone extensive optimization process as performed for V4. Applicability of the code for ship hydrodynamic problems have been demonstrated for flow around Athena bare hull at Fr = 0.25 and 5415 at Fr = 0.28. Large-scale calculations performed using V6 include a LES simulation for 5415 (Fr = 0.41) using a 262M grid on 1024 processors and a RANS simulation using 100M grid points for 5415 (Fr = 0.28) on 144 processors on NAVO's IBM P5 (Babbage).

V4 is currently the work horse code at IIHR for ship resistance, propulsion, seakeeping and maneuvering calculations. The code has several simulation based

design (SBD) functional areas and shows reasonable scalability. A semi-coupled two phase flow version of the code is available where the air phase is solved using water velocity as boundary condition [14]. The thermal and solute transport equations are implemented assuming a weakly compressible approximation for air flow. The approach has been used to study the dynamics of exhaust smoke and thermal plume from stacks of ONR tumblehome. Previously, a fully-coupled two-phase flow version of the code was developed using coupled ghost-fluid/Heaviside level-set methods which had limitations for overset grids [15]. Recently the code was modified by implementing geometry based level-set methods applicable for highly distorted grids. However, this approach too has limitations for dynamic overset grids and requires smaller time step than V4. In the long term, the semi-coupled two-phase solver and its functional areas will be added to V4. Future development for V4 will focus on reducing memory requirements by implementing Cartesian grid solver for background and refinement blocks. However, accuracy and scalability limitations of V4 are the bottleneck in applicability of this code to large-scale calculation using billions of grid points. Further, for simulations with dynamic motions the scalability of V4 is limited by the SUGGAR interpolation.

In contrast, V6 is a research code which is being turned into a ship hydrodynamics code. The code has been previously applied to several fundamental problems such as wave breaking, bubble entrainment and air layer drag reduction where it performs better than V4. An orthogonal curvilinear grid solver is under development which will replace wall-layer modeling using WF. The boundary layer orthogonal curvilinear grid will be coupled with background Cartesian grid using overset grid approach with strong and weak pressure coupling. It is expected that orthogonal curvilinear grids will have limitations for complex geometries for which non-orthogonal grids may be used with deferred corrections for non-orthogonality. Future work includes development of a hybrid structured/ unstructured grid solver where the structured boundary layer curvilinear and background Cartesian grids will be stitched using unstructured grids, thereby avoiding scalability limitations due to SUGGAR.

CFDSHIP-IOWA HPC OPTIMIZATION AND SCALABILITY STUDY

Naval Oceanographic Office (NAVO) Major Shared Resource Center (MSRC) established HPC modernization program in early 1990's[16]. Earlier computational facilities consisted of 8 processor Cray YMP with peak computational capability of 3.2GFlops **(**FLoating point Operations Per Second). In early 2000, HPC capabilities were extended to 256 processor with peak computing of 3.2TFlops and bandwidth (data rate supported by network connection) of 622Mbps (bits per second). Babbage was added in 2006-2007 which consisted of 192 nodes with 16 CPUs/node (3072 processors) with 32GB memory per node, processor clock speed of 1.9GHz, peak computation capability of 22TFlops, single port bidirectional bandwidth of 2.9Gbps and latency (time taken by memory to respond to a request from the CPU) of 7-14 microseconds. Late 2008 significant upgrades were performed in HPC capabilities which included DaVinci IBM P6 and Einstein CRAY XT5 systems. DaVinci consists of 166 nodes with 32CPUs/node (5312 processors) with 64GB memory per node, processor clock speed of 4.7GHz, peak computation capability of 90TFlops, single port bidirectional bandwidth of 3.8Gbps and latency of 140-240 nanoseconds. Einstein

consists of 1660 nodes with 8CPUs/node (12872 processors) with 16GB memory per node, processor clock speed of 2.3GHz, peak computation capability of 117TFlops and single port bidirectional bandwidth of 6.4Gbps. The following scalability studies were performed as part of the Capabilities Application Project (CAP) effort which allowed selected large scale computational applications to be run on significant portion of the HPC systems for a short period of time before these machines were released for application.

CFDShip-Iowa V4

Recently, Carrica et al. [9] improved V4 HPC performance by optimizing serial and parallel execution of routines and overset grid assembly. Extensive profiling was performed using PETSc facility of user-defined events to identify bottlenecks of the in-processor and inter-processor procedures. Several inefficient routines were identified and rewritten resulting in up to 10 times speedup for large cases. Parallel optimizations include elimination of unnecessary MPI barriers, use of collective MPI instructions whenever possible, and parallel I/O. Memory usage was improved to avoid using shared memory and allow scalability on distributed memory machines. For this purpose a scalable PDE-based reinitialization was added as an alternative to the geometrical reinitialization. To optimize the overset assembly, SUGGAR was implemented as a library which can be executed on a dedicated MPI rank rather than running it as a separate process with synchronized communication with V4. This eliminated the I/O and the associated overhead and resulted in 20% lower CPU time. Several options were added to SUGGAR to improve the execution speed for moving body problems, such as limiting the grids to be searched for donors, special management for Cartesian grids, reusing the donors from the previous time step to initialize the donor search, preassembly of dynamic grid groups which will be static through the computation, and use of threads to perform various parts of the overset grid assembly in parallel. The donor reuse increased the memory usage which was somewhat reduced by using pre-assembly. The performance of the optimized code was evaluated for 5415 and KVLCC simulations with static and dynamic overset on grids ranging from 5.6M to 115M points.

Herein, strong scalability tests are performed for fixed sinkage and trim 5415 ($Re = 4.85\times10^6$, $Fr = 0.28$) using a 115M grid on DaVinci and Einstein. Weak scalability test were performed by Carrica et al. [9] on Hawk for fixed sinkage and trim KVLCC and 5415 geometries using 120K and 240K grid points per processors, respectively. Fixed sinkage and trim cases were chosen to avoid SUGGAR interpolation every time step. The solver CPU times are based on average of 10 time steps using 5 inner-iterations for pressure-velocity coupling without I/O.

As shown in Fig 1(a), V4 scales almost linearly from 256 to 1024 processors where scalability is 16.7% and 9.8% below ideal scaling on Einstein and DaVinci, respectively. The speedup drops 37% below ideal scaling for 2048 processor on Einstein. On Hawk the speedup is observed to be 23% below ideal scaling even for 512 processors. CPU times without I/O on DaVinci is observed to be 10-15% lower than that on Einstein for 512 and large processors runs. As shown in Figure 2(a) about 71% of the CPU time is spent for solving the pressure Poisson equation, 18.2% for turbulence, 6.5% for interface tracking and 4.3% for the momentum equations. The I/O time using single processor increases by about 15% as the number of processors is

increased from 256 to 2048 as shown in Fig. 3. The I/O time on Einstein is almost 50% lower compared to that on DaVinci. MPI I/O does not show significant improvement in I/O times.

A fairly good weak scalability is observed up to 500 processors as shown in Fig. 1(b), even for different problems and for grid points per processor ratio of 2:1. The deviation from the ideal scaling for one of the cases using 115M grid points was attributed to the saturation of memory on each 500-processor node. The case with 128 processors uses PISO solver which is more expensive than the standard Projection algorithm used for other cases, this causes a deviation for weak scalability [9].

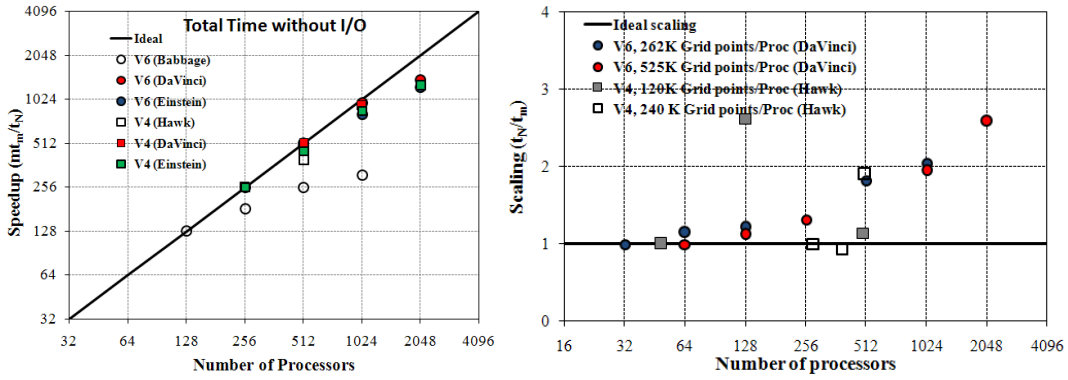

(a) (b)

Figure 1. (a) Strong scalability of total times without I/O for V4 and V6 are compared with ideal scaling. (b) Weak scalability tests using 120K and 240K grid points per processor for V4 and 262K and 525K grid points per processor for V6. Tests are performed on NAVO Cray XT5 (Einstein), NAVO IBM P6 (DaVinci), NAVO IBM P6 (Babbage)[13] and AFRL SGI Altix 4700 (Hawk) [9].

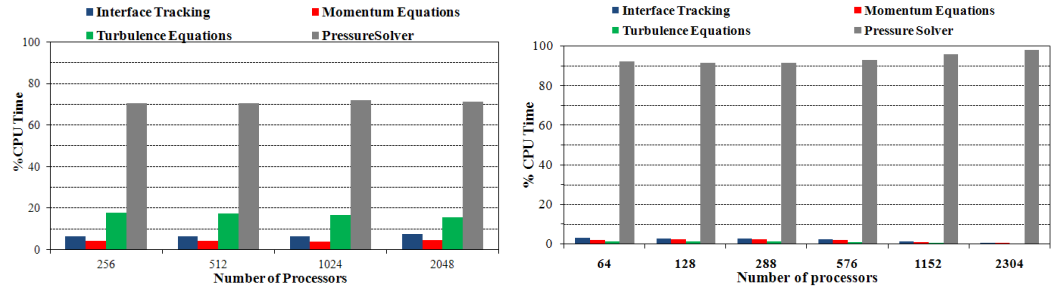

(a) (b)

Figure 2. % CPU time required for several components of the CFDShip-Iowa for 5415 simulation using (a) V4 for a 115M grid on NAVO Cray XT5 (Einstein), and (b) V6 for a 100M grid simulation.

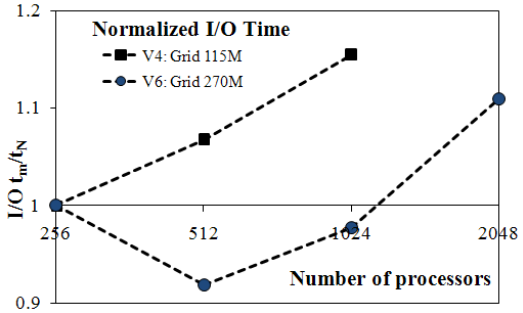

Figure 3. % I/O time required for CFDShip-Iowa on NAVO Cray XT5 (Einstein). V4 uses I/O using single processor, V6 uses MPI I/O.

CFDShip-Iowa V6

Recent developments in HPC were performed by Yang et al. [13]. They extended the one-dimensional slab decomposition to three directions for parallelization. The inter-processor communications for ghost cell information exchange were changed into non-blocking mode. Parallel I/O using MPI2 was implemented such that all processors read from and write to one single file instantaneously. This approach is much more effective than one or a few processors receive data from all processors and write to one or a few files, and more convenient than every processor writes its own data files. It was identified that the load balance on each processor is affected by the uneven distribution of the overheads due to interface and immersed boundary treatment.

Strong scalability tests are performed for fixed sinkage and trim 5415 (Re = 4.85×10^6, Fr = 0.28) using 100M (Grid#1), 270M (Grid#2) and 540M (Grid#3) grids on DaVinci and using Grid#2 on Einstein. Weak scalability tests are performed using 262K and 525K grid points per processor on DaVinci. The solver CPU times are based on average of 10 time steps without I/O.

As shown in Fig. 1(a), V6 scales linearly up to 512 processors for Grid#1 and 1024 processors for Grids#2 and #3. In the 2048 processor case the scalability drops 25% and 33% below ideal scaling for Grid#3 and Grid#2, respectively. As expected, the scalability of the code improves when the grid size increases, i.e., number of grid points per node are sufficiently large. The scalability on DaVinci is about 4% better than that on Einstein and significantly better than that on Babbage. On Babbage the performance drops by 20% even with 256 processors for a 270M grid. CPU time for DaVinci is observed to be 30-33% lower than that on Einstein. As shown in Fig. 2(b), almost 92% of the CPU time is spent for the pressure solver, 3% for interface tracking, 2.5% for momentum equations and 1.2% for turbulence equations. The momentum, turbulence and interface tracking solvers show linear scalability. Thus scalability of the code is determined by the scalability of pressure Poisson solver. MPI-I/O times do not scale with number of processor and vary by only 10-11% as shown in Fig. 3.

In theory, a weak scaling factor of 1 should be expected as each processor handles the same amount of data. However, Fig. 1(b) shows that the CPU time increases with the number of processors. The deviation from ideal scaling is mainly affected by HYPRE. HYPRE is a semi-coarsening multi-grid solver in which the semi-coarsening process is performed down to a 1×1×1 grid. Thus for finer grids extra levels of coarsening have to be performed for finer grids leading to extra computational cost.

Discussion

Scalability performances of the codes are 5-10% better on DaVinci compared to Einstein. CPU times are 10-15% and 30-33% lower on DaVinci compared to Einstein for V4 and V6, respectively. Performance improvement is expected on DaVinci as its compute capability/processor and processor speed is almost twice of Einstein. However, the performance improvement is significantly lower than expected value of 100% especially for V4. DaVinci is also better than Einstein in terms of memory/node. On Einstein memory saturation restricted use of only 75%

processors/node for V4 for 256 processor case. Overall, it is estimated that almost 40% and 60% lower CPU time is required on DaVinci compared to Einstein for V4 and V6, respectively. MPI I/O does not show significant improvement over single processor I/O and does not scale with #processors. I/O times were also significantly affected by other processes running on the login (MOM) node. I/O times could be a bottleneck for large scale computations which requires frequent I/O to obtain vortical and turbulent statistics.

V4 scalability drops by 37% below ideal scaling on 2048 processors compared to 25-30% drop for V6. Memory requirements for V4 are almost twice of V6. Weak scalability shows that the best results using V4 and V6 are obtained using 240K and 525K grid points per processors, respectively. Thus it can be estimated that the largest simulation using V4 and V6 can be performed using 490M and 1billion grid points, respectively. The main scalability bottle neck is identified to be the pressure Poisson solver. Scalability of other codes is not readily available, here we compare with the limited studies available in the literature. Results obtained using CFDShip-Iowa are reasonable when compared to Fluent, which shows 20% drop in speedup on 240 processors for auto aerodynamics using 29M grid points on SGI 2800/SSI platform [17]. As expected, Gicquel [18] has shown almost ideal speedup up to 4000 processors for compressible flow code for turbulent combustion problem using 40M grid points where solution of pressure Poisson equation is not required.

Scalability of V4 is restricted by the solver architecture. Further improvement in V4 HPC performance can be obtained by introducing Cartesian solver for background and refinement blocks. Simulations involving ship motions require SUGGAR call every time step. Thus, for dynamic motions, V4 is scalable only up to the number of processors for which the time required for CFD solver is greater than or equal to the time required for SUGGAR. For V6 around 92% of the solver time is spent in HYPRE. This suggests that other components of the solver are well optimized thus HPC improvements should focus towards optimizing HYPRE. HYPRE can be optimized by avoiding matrix reconstruction and reconditioning every time step, switching off residual calculation etc. Future simulations will be performed in close collaboration with software experts at ANL to address the scalability limitations of PETSc and HYPRE.

5415 WITH BILGE KEELS AT 20° STATIC DRIFT CONDITION USING V4

SIMMAN workshop [19] included validation of 5415 at 10° static drift for which comparison error E=D-S, where D is EFD and S is solution, were 15.2%D, 3.0%D and 8.2%D for longitudinal force X_t, sway force Y_t and yaw moment N_t coefficients, respectively. Sakamoto [20] performed calculations for 5415 at 10° and 20° static drift and obtained E up to 12%D, 11%D and 2%D for X_t, Y_t and N_t, respectively. Sensitivity studies were performed using ARS, BKW and DES turbulence models and using fine grids up to 20M, which showed minimal improvements. One possibility for error was thought to be due to the absence of transition modeling in turbulence equations. Based on the URANS simulation here we construct a grid which has sufficient density to activate DES properly as shown in Fig. 5. E reduces significantly on this grid presumably due to correct prediction of cross-flow separation.

URANS/DES simulations are performed using BKW for fixed sinkage and trim 5415 with bilge keels at 20° static drift condition Re=4.85×106, Fr=0.28. The verification study is performed following the quantitative methodology and procedures proposed by Stern et al. [21] and recent modifications proposed by Xing and Stern [22] using three systematically refined grids with $r_G = \sqrt{3}$ consisting of 10M, 48M and 250 M points. The grid design is shown in Fig. 4(a). The sinkage = 1.92×10^{-3} and trim = 0.136° values are based on EFD data [23]. Hybrid $1^{st}/2^{nd}$ order scheme is used for level-set equations. Hybrid $2^{nd}/4^{th}$ order upwind scheme is used for the convection term in DES, whereas 2^{nd} order upwind scheme is used in URANS. The projection algorithm is used to satisfy continuity. The 250M grid simulation is performed on 1212 processors with a time step size of 2.5×10^{-3} seconds. The memory required for this case is around 430GB. The simulation is performed for 3.55 flow times which requires about 96 hours of clock time and 150K CPU hours. The results are compared with the URANS and DES results obtained using a 7M grid [20] and EFD data [23].

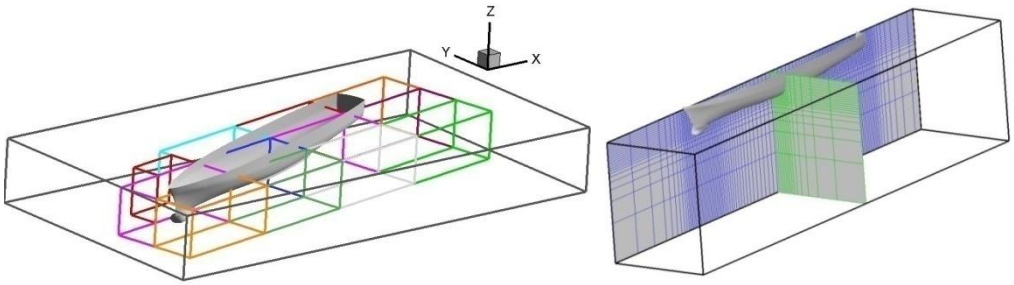

(a) (b)

Figure 4. The domains for the 5415 simulations, Fr=0.28, $Re=4.85\times10^6$ at: (a) 20° static drift using V4 and (b) static straight ahead using V6.

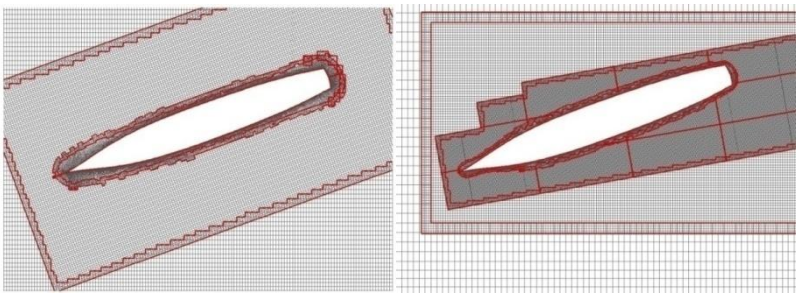

(a) 7.0 M Grid (b) 10 M Grid

Figure 5. A X-Y cross-section showing the grids used in (a) URANS/DES simulation using 7 M grid and (b) URANS/DES simulation using10 M grid.

Verification study for longitudinal frictional (X_f), pressure (X_p) and total (X_t) coefficients, sway frictional (Y_f), pressure (Y_p) and total (Y_t) coefficients, and frictional (N_f), pressure (N_p) and total (N_t) yaw moment coefficients are summarized in Table 1. $U_I \leq 0.75\%$ for the resistance and moment coefficients on all the grids, which are estimated from the dynamic range of the running mean fluctuations, obtained using 2.5 flow time solutions after the transient. To avoid contamination of

grid uncertainty (U_G) by U_I, it is required that U_I is one or two order of magnitudes lower than ε_{12}. For frictional coefficients $U_{I,1}/\varepsilon_{12} < 0.12$, whereas for pressure coefficients $U_{I,1}/\varepsilon_{12} > 2.7$. For N_p and N_t, ε_{23} is of the same order of U_I which causes ε_{12} to increase by 3 times of ε_{23}. Similar results were obtained by Xing et al. [2] for bare hull Athena verification study. Monotonic convergence $R_G < 0.52$ is obtained for X_f, X_p and X_t, oscillatory convergence $-0.62 < R_G < 0.12$ for Y_f, Y_p and Y_t, oscillatory divergence for N_f, and monotonic divergence for N_p and N_t. The correction factor (CF) < 0.65 for X_f, and X_t, whereas CF=16.5 for X_p which is considered to be divergent. The observed order of accuracy (P_G) for X_t is 3.29 which is close to theoretical order of accuracy (P_{Gth}) of 4. U_G is 3.25% for X_f and < 1% for X_t and sway resistance coefficients.

The 7M grid URANS and DES results over predict X_t and Y_t by 13-16% and 9-11% compared to the EFD data, respectively. N_t compares well within 2.7% of EFD data for both the cases. In the 10M URANS and DES simulations X_t and Y_t are over predicted by 8.77% and 5.22%, respectively. For this grid too, N_t is predicted within 2.8% in both the cases. The 48M grid results are predicted within 4% and 1% of EFD data for resistance coefficients and N_t, respectively. 250M grid shows errors up to 5.3% for resistance coefficients and 1.35% for N_t. DES shows 4-5% lower E than URANS, and the best results are obtained on 48M grid where E<4%D. EFD uncertainties (U_D) are 7.9% for X_t, 4.1% for Y_t and 1.30% for N_t. The validation uncertainty (U_V) is computed to be 7.92% for X_t and 4.21% for Y_t. The error defined as the difference between fine grid simulation and EFD (E) is 4.57% < U_V for X_t, and E = 3.72% < U_V for Y_t. Thus both X_t and Y_t are validated. $E \leq 1.82\%$ for N_t on all grids, which is slightly larger than U_D=1.3%. Results show $U_G << U_D$, which suggests errors are dominated by modeling errors.

Table 1. Resistance and moment coefficients prediction and DES verification study for 5415 with bilge keels at 20° static drift condition.

Parameters	EFD	DES Verification Study			ε_{23}%	ε_{12}%	$U_{I,1}$%	$U_{I,1}/\varepsilon_{12}$	R_G	P_G	CF	U_G%	U_D%	U_V%
		Grid3 10M	Grid 2 48M	Grid 1 250M										
$X_f \times 10^2$	-	-1.389	-1.418	-1.434	2.14	1.11	0.10	0.090	0.516	1.21	0.12	3.25		
$X_p \times 10^2$	-	-1.492	-1.561	-1.562	4.42	0.03	0.70	23.33	0.008	8.90	16.5	-		
$X_t \times 10^2$	-2.865	-2.879	-2.979	-2.996	3.33	0.55	0.38	0.691	0.164	3.29	0.64	0.44	7.9	7.92
	$\%E_X$	**+0.49**	**+3.98)**	**+4.57**	-									
$Y_f \times 10^2$	-	0.116	0.127	0.121	8.60	5.29	0.62	0.117	-0.615	-	-	0.99		
$Y_p \times 10^2$	-	1.597	1.569	1.573	1.76	0.26	0.70	2.692	-0.146	-	-	0.63		
$Y_t \times 10^2$	15.29	16.088	15.821	15.860	1.68	0.22	0.74	3.364	-0.128	-	-	0.63	4.1	4.21
	$\%E_Y$	**+5.22**	**+3.47**	**+3.72**	-									
$N_f \times 10^2$	-	0.013	0.015	0.012	17.7	28.5	0.40	0.025	-1.607	-	-	-		
$N_p \times 10^2$	-	6.029	5.982	5.843	0.81	2.37	0.70	0.295	2.92	-	-	-		
$N_t \times 10^2$	5.935	6.042	5.997	5.855	0.77	2.42	0.70	0.289	3.13	-	-	-	1.3	
	$\%E_N$	**+1.82**	**+1.05**	**-1.35**	-									

$\varepsilon_{23}=|(S_2-S_3)/S_1|\times 100$; $\varepsilon_{12}=|(S_1-S_2)/S_1|\times 100$

In Fig. 6 the time histories and FFTs of X_t, Y_t and N_t are compared with EFD data. As evident, the URANS coefficients are almost steady and the unsteadiness of the signal grows with grid refinement in DES. The 250M grid simulation shows large amplitudes for higher frequencies up to f = 40. The amplitudes of the oscillations are underpredicted for X_t and over predicted for Y_t and N_t when compared with the EFD data. FFT of X_t in the 250M grid simulation shows two dominant frequency zones,

first around τ=0.05 and second around τ=0.1. Peaks amplitudes at 0.05 and 0.1 periods are observed in EFD data too. Experimentalists [23] attributed these frequencies with the noise from carriage speed vibrations τ=0.05 and load-cell τ=0.1.

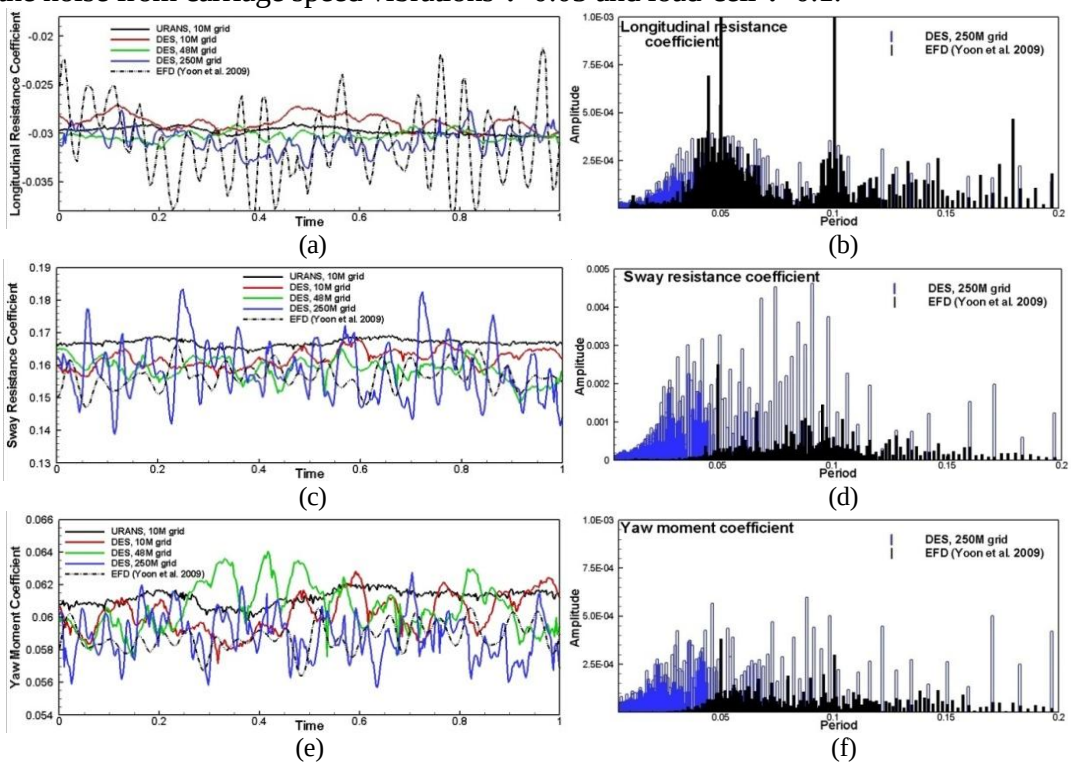

Figure 6. Time history and FFT of (a),(b) longitudinal resistance, (c),(d) sway resistance and (e),(f) yaw moment coefficients obtained DES simulations are compared with EFD data [23].

Free surface elevation shows asymmetric pattern dominated by bow and stern waves. Diverging waves are observed on both starboard and port side, and transverse wave is observed on port side between diverging waves and hull. Overall the wave patterns are similar on all the grids. The free-surface scar on port side close to the hull and the bow wave breaking patterns on both port and starboard sides are resolved better on finer grids as shown in Fig. 7(a,b). The wave envelop half angle α_{env}=10° and 40° on starboard and port sides, respectively. For β=0°-10° simulations, α_{env}= 19° is almost same on both starboard and port sides. Port side diverging waves has more pronounced troughs and starboard side diverging waves have higher peaks than β=0° case. Isosurfaces of Q in Fig. 7(c,d) for 10M grid shows sonar dome, bilge keel, aft-body keel, and port and starboard free-surface vortices. The sonar dome vortex exhibits helical instability breakdown. Kelvin-Helmholtz, Karman and flapping-type instabilities are observed on the leeward side. In the 250M grid simulation sonar dome vortex is clearly visible, but the other vortices are masked by the massive cross-flow separation. Further analysis is required to obtain frequency and scaling of these instabilities.

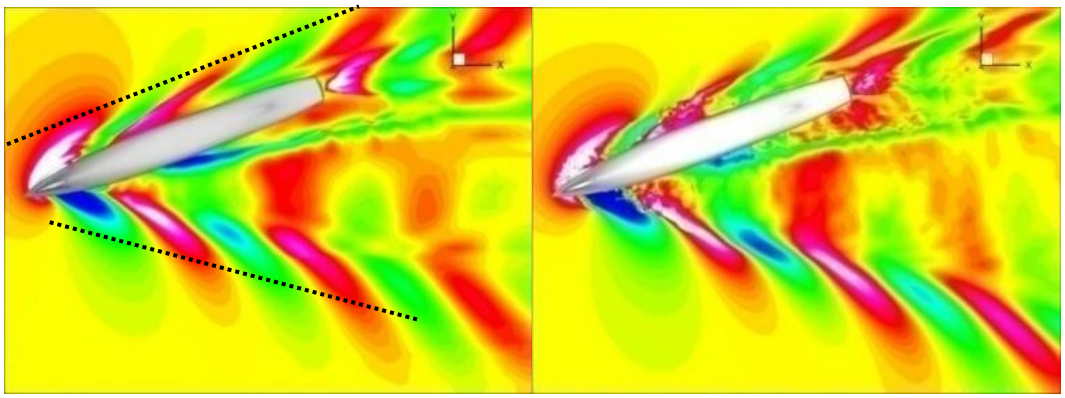

(a) 10 M grid DES (b) 250M grid DES

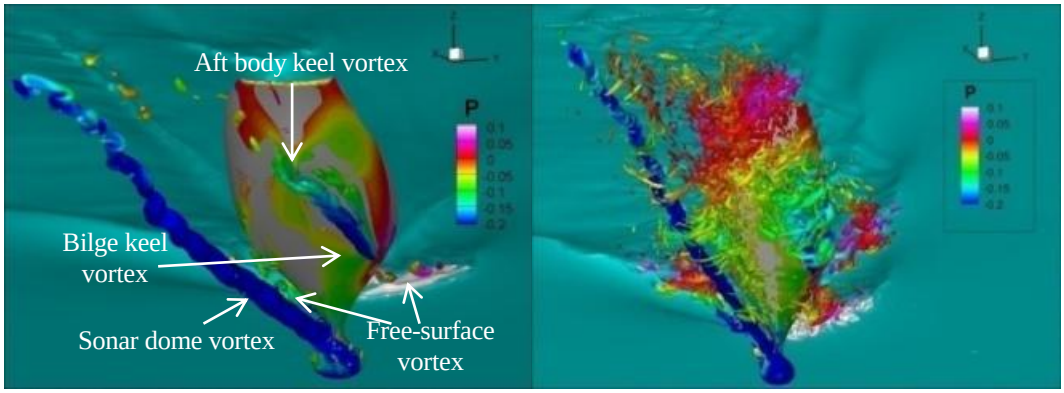

(c) 10M grid DES (d) 250M grid DES

Figure 7. (a), (b) Free-surface wave elevation and (c), (d) isosurfaces of Q=1000 obtained for static 20° drift 5415 DES simulations using 10M grid and 250M grids. Wave elevation contour levels are from -0.01 to 0.01 with intervals of 4×10^{-4}.

5415 BARE HULL AT STRAIGHT AHEAD CONDITION USING V6

Previously 5415 bare hull at straight ahead condition $Re = 4.85\times10^{6}$, $Fr = 0.28$ was studied by Wilson and Stern [24] using CFDShip-Iowa V3 which uses surface-tracking method for free-surface modeling. The study focused on the verification and validation of resistance prediction, wave profile and velocity profile at nominal wake plane using the EFD data [25], where the finest grid consisted of 1.78M points. The boundary layer and wake profile were compared with the EFD data at $Fr = 0.28$ but higher $Re = 1.2\times10^{7}$ [26], and the fine grid turbulent kinetic energy (TKE) and Reynolds stress profiles at nominal wake plane (x/L = 0.935) were compared with Longo et al. [25] EFD data. The resistance, wave elevations and boundary layer profiles were validated within 6.4% uncertainty. The boundary layer and wake profiles showed over prediction of sonar dome vortex and boundary layer profile at nominal wake plane, and the stern bilge vortex was not captured at mid-girth section. The normal and shear stress profiles were predicted well qualitatively, however only the magnitudes of $u'u'$ and $u'v'$ were predicted correctly. Normal stresses $v'v'$ and $w'w'$ were overpredicted resulting in over prediction of TKE. Recently, Sakamoto et al. [20] studied the effect of BKW and ARS turbulence models and 2nd order upwind and TVD convective schemes on resistance prediction using V4 on a 1.27M grid. They

obtained significant improvements in the results using ARS model, however the effect of convective scheme was inconclusive.

Herein, simulations are performed for 5415 bare hull at straight ahead condition $Re = 4.85\times10^6$, $Fr = 0.28$ using V6-WF with BKG at fixed sinkage=1.92×10^{-3} and trim=0.136°. The corresponding Re for the air flow is 3.23×10^5. The simulations are performed for the half ship-hull using three grids: 1024×128×256 (34M) with y^+=150, 1800×200×256 (92M) with y^+ = 60 and 2400×288×400 (276M) with y^+ = 30. The surface grid consists of 84K elements. The grid design for the simulation is shown in Fig. 3(b). 5th order WENO scheme is used for both level-set equation and convection terms. The pressure Poisson equation is solved using the multi-grid HYPRE solver. The 276M grid simulation is performed on 384 processors with time step size of 1.75×10^{-5} with periodic time striding [27], i.e., time step size is increased to 8.75×10^{-5} every 10th time step. The memory requirement for this case is approximately 250GB. The simulation is performed for 1.53 flow times which requires about 900 hours of clock time and 350K CPU hours. V6-WF results are compared with half ship-hull V4-BKW, V4-WF results on 615K grid, V4-DES on 300M grid and EFD in Figs. 8-12.

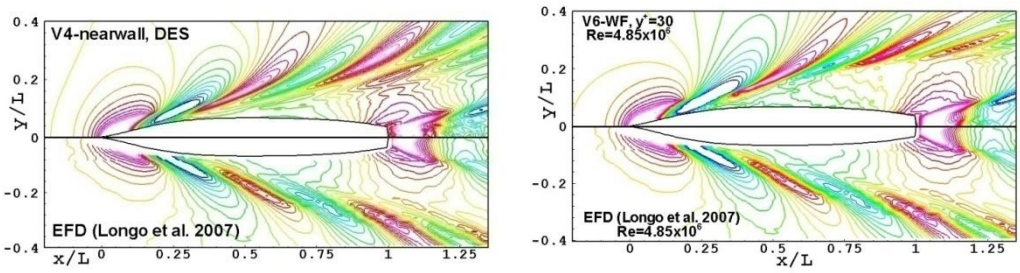

Figure 8. Wave elevation profiles for 5415 obtained using V4-DES and V6-WF with y^+=30 are compared with EFD data. Contours levels are from -5×10^{-3} to 5×10^3 with intervals of 5×10^{-4}.

V4-BKW over predicts resistance coefficient by 5.6%*D*, V4-WF predictions are within 2%*D* and V4-DES results are within 2.6%*D*. The poor V4-BKW predictions could be due to the coarse grid resolution as Sakamoto [8] has shown errors less than 3% on a 1.27M grid. Further study is required using finer grids to obtain V4-BKW and V4-WF benchmark solutions. The wave elevation patterns are predicted well in both V4 and V6 simulations on all the grids when compared with the EFD data. The wave pattern resolution improves with grid refinement. V4-DES and V6-WF with y^+ = 30 results are in detailed agreement with EFD.

EFD mean flow pattern shows interactions between the hull boundary layer and sonar dome (near center plane) and after body shoulder (near mid girth) out-board rotating axial vortices. For the nominal wake plane, inboard of the axial vortex center and near the center plane, high momentum fluid is transported towards the hull thinning the boundary layer, whereas outboard of the vortex center low momentum fluid is transported away from the hull causing bulge in the boundary layer. The mean and turbulent nominal wake flow pattern shows similarity to the boundary layer and turbulence structures in the presence of common-down streamwise vortex pair. V4-BKW predicts the sonar dome rotating vortex and its interaction with boundary layer fairly well. However, the sonar dome vortex is over predicted at development and the after body shoulder vortex is not resolved well suggesting rapid dissipation of the vortex. At the nominal wake plane the boundary layer is thicker at center plane

compared to the EFD data and the bulge is underpredicted due to weak vortex strength. The TKE and stress contours compare well with EFD qualitatively but not quantitatively. V4-WF predictions are similar to that of V4-BKW for mean velocity profiles, but has penalty in prediction of turbulence quantities. V6-WF results improve with decrease in y^+ and has penalty similar to V4-WF. V6-WF with y^+=30 over predicts the bilge vortex strength significantly resulting in over prediction of boundary layer bulge. TKE peak is observed to be at the center plane compared to *y/L*=0.01 in EFD and the peak value is overpredicted by about 40%. Both normal and shear stresses are also over predicted. Preliminary analysis of the V4-DES instantaneous solution shows that it captures the co-rotating vortices at mid-girth and the bulge of the streamwise velocity is predicted better than V4-BKW at nominal wake plane.

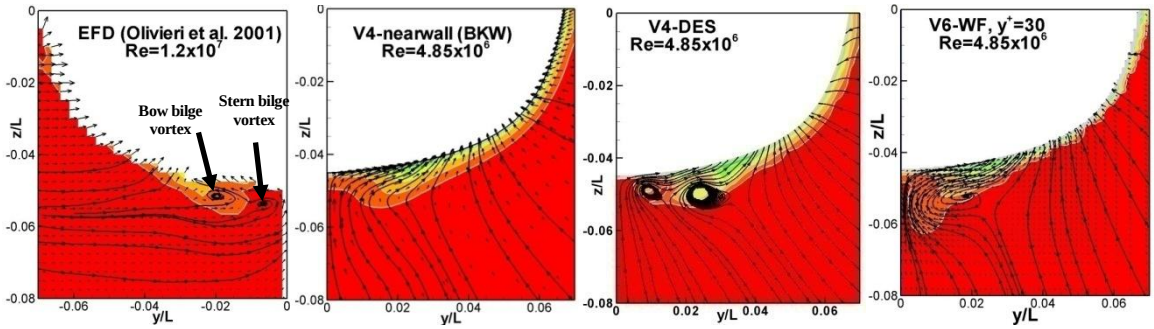

Figure 9. Boundary layer and wake profiles at x/L = 0.6 obtained using V4-BKW, V4-DES and V6-WF with y^+ = 30 are compared with EFD data [24]. Streamwise velocities are shown with filled contours and (GREY) lines, and cross flow is shown using vectors and streamlines (Black lines).

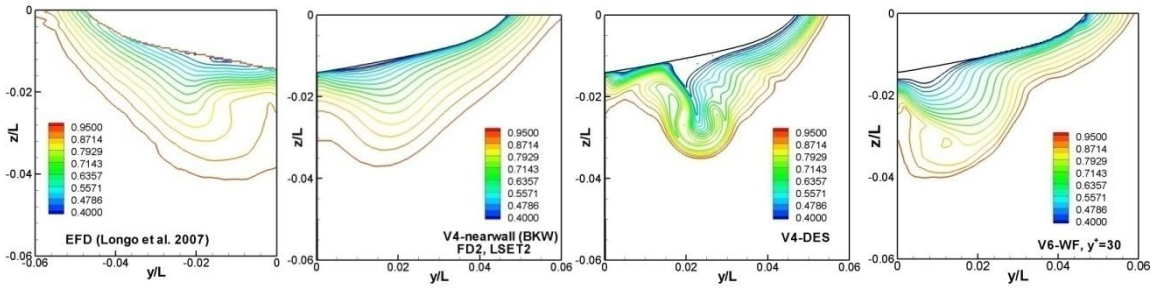

Figure 10. Boundary layer profile at x/L = 0.935 obtained using V4-BKW, V4-DES and V6-WF with y^+ = 30 are compared with EFD data [24].

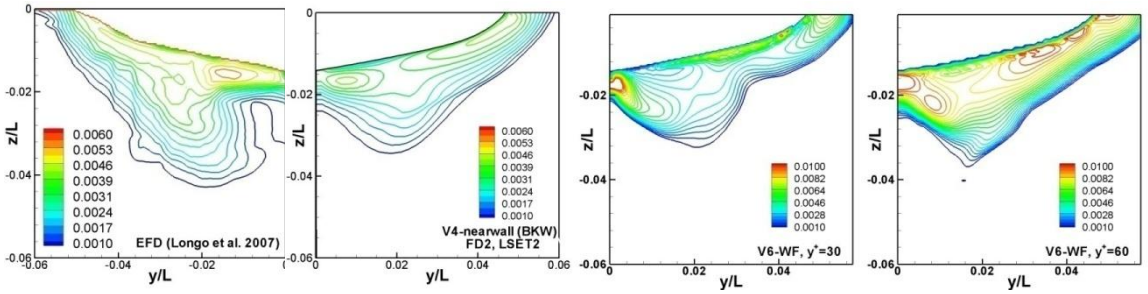

Figure 11. The turbulent kinetic energy distribution on the nominal wake plane (x/L=0.935) obtained using V4-nearwall, V4-WF and V6-WF are compared with EFD data [23].

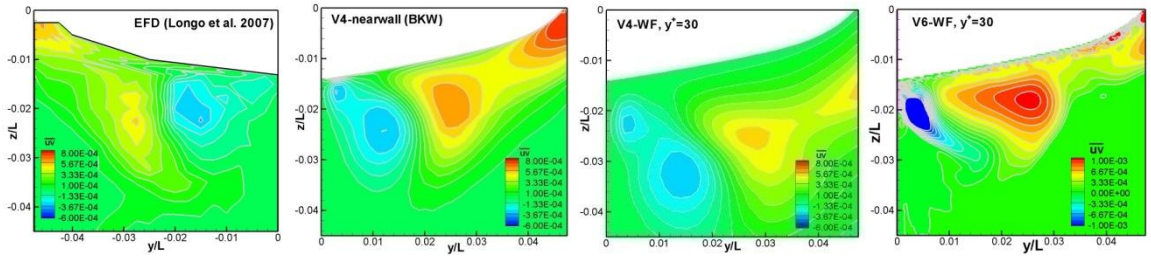

Figure 12. Shear stress u′v′distribution on the nominal wake plane (x/L=0.935) obtained using V4 near-wall, V4-WF and V6-WF are compared with EFD data [23].

CONCLUSIONS

V6 has advantages over V4 both for accuracy and high performance computing (HPC). V6 is more accurate as it provides better mass conservation, allows implementation of higher order schemes and better surface capturing models such as VOF easier than V4. V6 is better for HPC as the memory requirements and CPU time/time-step/processor/grid-point for V6 are estimated to be around 50% and 20-25% of those for V4 for a similar size grid, respectively. V6 is scalable up to 2048 processors where the speedup drops by 25% below ideal scaling compared to 37% in V4. It is estimated that 490M and 1billion grid points are the largest grid that can be used for V4 and V6 calculations on … computing platforms at present, respectively. The main scalability bottle necks are identified to be the pressure Poisson solver, I/O and SUGGAR grid interpolation. Future simulations will be performed in close collaboration with software experts at ANL to address the scalability limitations of PETSc and HYPRE. Development of a domain decomposition version of SUGGAR is required to remove scalability limitations of V4 for dynamic motions.

V4-DES V&V study for 5415 with bilge keels at 20° static drift simulation shows grid convergence with $U_G < 3.5\%S_1$ for both X_t and Y_t, which are validated within $5\%D$ uncertainty. FFT of force and moment coefficients show dominant frequency at τ=0.05 and 0.1. These dominant frequencies are also observed in the EFD, but were attributed to experimental noise. The 250M grid results show massive cross-flow separation and highly unsteady wave pattern with bow-wave breaking. Further analysis of the volume solution will be performed to study instantaneous and mean separation flow patterns, to identify the dominant frequencies in resistance and moment coefficients with vortical structures and instabilities and the source of the free-surface scars. TKE distribution and its budget, and Reynolds stress distribution will be analyze to understand the 3D turbulent structures for ship flows. This study will complement the previous studies for Athena [28] and KVLCC [29]. Future work includes verification study using intermediate grids to reduce CF values. In order to reduce U_I more non-linear iterations of pressure velocity coupling and/or implementation of more accurate and efficient iterative methods are required. EFD is planned with reduced experimental noise to obtain better measurements of the hydrodynamics response on resistance coefficients.

In the 5415 at straight ahead simulation, both V4-DES and V6-WF provide detailed agreement of the wave pattern. V4-BKW provides reasonable results for the mean velocity, TKE and stress profiles, but fails to predict the sonar dome vortex strength accurately. WFs show penalty in flow prediction both in V4 and V6, where

the latter shows the worst comparison with EFD. Best results using WFs are expected with y^+=30, thus it can be concluded that wall-layer modeling using WF for IBM has limitations for complex geometries. Preliminary V4-DES results show significant improvements over the V4-BKW. Mean flow will be obtained from V4-DES to identify the mean vortical structures, and the turbulence quantities at nominal wake plane will be compared with EFD data. Future work includes validation of force computations using V6 and obtaining V4-BKW and -WF benchmark solutions on appropriate grid.

V6 is better suited for large scale computation compared to V4. However, V6 has some limitations such as: (1). Time step size is very small compared to V4, (2). IBM requires very fine grids to resolve the boundary layer and local grid refinement cannot be performed, and (3). Wall-layer modeling using WF is not accurate for ship flows. Future development of V6 will address these limitations including development of weakly and strongly coupled wall layer (curvilinear orthogonal and non-orthogonal grids) with Cartesian background grid and implementation of SBD functional areas. In the long term V6 has the potential to develop into an efficient and robust general-purpose solver.

ACKNOWLEDGEMENTS

The research is sponsored by the Office of Naval Research under Grant N00014-01-1-0073 and N00014-06-1-0420, administered by Dr. Patrick Purtell. The computations were performed at DoD NAVO HPC machines.

REFERENCES

1. Carrica, P. M., Wilson, R. V., and Stern, F. 2007. "An Unsteady Single-phase Level Set Method for Viscous Free Surface Flows," *International Journal of Numerical Methods in Fluids*, 53(2): 229–256.
2. Xing, T., Carrica, P.M., and Stern, F. 2008. "Computational Towing Tank Procedures for Single Run Curves of Resistance and Propulsion," *Journal of Fluids Engineering*, 130, 101102: 1–14.
3. Xing, T., Kandasamy, M., and Stern, F. 2007. "Unsteady free-surface wave-induced separation: analysis of turbulent structures using DES and single-phase level-set," *Journal of Turbulence*, 8 (44): 1–35.
4. Bhushan, S., Xing, T., Carrica, P.M., and Stern, F. 2009. "Model- and full-Scale URANS simulations of Athena resistance, powering and seakeeping, and 5415 maneuvering," *Journal of Ship Research*, 53(4):179–198.
5. Carrica, P.M., Wilson, R.V., Noack, R. and Stern, F. 2007. "Ship Motions Using Single-Level Set with Dynamic Overset Grids," *Computers and Fluids*, 36(9):1415–1433.
6. Noack R. 2005. "SUGGAR: a General Capability for Moving Body Overset Grid Assembly," *17th AIAA Computational Fluid Dynamics Conference*, Toronto, Ontario, Canada.
7. Carrica, P.M., Paik, K.J., Hosseini, H.S., and Stern, F. 2008. "URANS analysis of a broaching event in irregular quartering seas," *Journal of Marine Science and Technology*, 13(4): 395–407.
8. Ismail, F., Carrica, P.M., and Stern, F. 2008. "Evaluation of Linear and Nonlinear Convection Schemes on Multidimensional Non-Orthogonal Curvilinear Grids-Part 1: Assessment on Analytical Benchmarks," *International Journal for Numerical Methods in Fluids*, DOI: 10.1002/fld.2174.
9. Carrica, P.M. et al. 2008. "Large-scale DES computations of the forward speed diffraction and pitch and heave problems for a surface combatant," *27th Symposium on Naval Hydrodynamics*, Seoul, Korea, 5–10 October.
10. Yang, J. and Stern, F. 2009. "Sharp interface immersed-boundary/level-set methods for wave-body interactions," *Journal of Computational Physics*, 228(17):6590–6616.

11. Wang, Z., Yang, J. and Stern, F. 2008. "An improved particle correction procedure for the particle level set method," *Journal of Computational Physics*, 228 (16):5819–5837.
12. Wang, Z., Yang, J., Koo, B., and Stern, F. 2009. "A coupled level set and volume-of-fluid method for sharp interface simulation of plunging breaking waves," *International Journal of Multiphase Flow*, 35 (3): 227–246.
13. Yang, J. et al. 2008. "Large-eddy simulation of ship flows with wall-layer models on Cartesian grids," *27th Symposium on Naval Hydrodynamics*, Seoul, Korea, 5–10 October 2008.
14. Huang, J., Carrica P.M., Mousaviraad, M. and Stern F. 2007. "Semi-coupled air/water immersed boundary approach in curvilinear dynamic overset grids with application to environmental effects in ship hydrodynamics," *Proc. of the 9th Intl. Conf. on Numerical Ship Hydrodynamics*, Ann Arbor, Michigan, Aug. 5-8, 83–101.
15. Huang, J., Carrica, P.M., and Stern, F. 2007. "Coupled ghost fluid/two-phase level set method for curvilinear body-fitted grids," *International Journal Numerical Methods Fluids*, 55: 867–897.
16. Cuicchi, C. 2009. "Navy DSRC retrospective: 1990-2009," *HPC Insights*, Spring Issue.
17. Kremenetsky, M. 2008. "Considerations for Parallel CFD Enhancements on SGI ccNUMA and Cluster Architectures," *http://www.fluent.com/software/fluent/fl5bench/otherart/oart1.htm*.
18. Gicquel, L.Y.M. et al. 2008. "Large eddy simulations of turbulent reacting flows in real burners: the status and challenges," *Journal of Physics: Conference Series*, 125, 012029.
19. Stern, F. and Agdrup, C. 2008. Proceedings of SIMMAN 2008 workshop on verification and validation of ship maneuvering simulation methods, Lingby, Denmark.
20. Sakamoto, N. 2009. "URANS and DES simulations of static and dynamic maneuvering for surface combatant," *Ph.D. thesis in preparation*, The University of Iowa.
21. Stern, F., Wilson, R. and Shao, J. 2006. "Quantitative approach to V&V of CFD simulations and certification of CFD codes," *International Journal of Computational Fluid Dynamics*, 50: 1335–1355.
22. Xing, T. and Stern, F. (2008). "Factors of Safety for Richardson Extrapolation for Industrial Applications," *IIHR Technical Report No. 466*.
23. Yoon, H.S. 2009. "Force/Moment and Phase-Averaged Stereo PIV Flow Measurements for Surface Combatant in PMM Maneuvers," *Ph.D. thesis in preparation*, The University of Iowa.
24. Wilson, R. and Stern, F. 2002. "Verification and Validation for RANS Simulation of a Naval Surface Combatant," *AIAA 2002-0904 Aerospace Sciences Meeting*, Reno, Nevada.
25. Longo, J., Shao, J., Irvine, M. and Stern, F. 2007. "Phase-averaged PIV for the nominal wake of a surface ship in regular head waves," *Journal of Fluids Engineering*, 129 (5): 524–540.
26. Olivieri, A., Pistani. F., Avanzini, A., Stern, F., and Penna, R. 2001. "Towing Tank Experiments of Resistance, Sinkage and Trim, Boundary Layer, Wake, and Free Surface Flow Around a Naval Combatant INSEAN 2340 Model," *IIHR Technical Report*, 421.
27. Sanmiguel, R-E., Ortega, C-J., and Fernandez F-R. 2003. "On the efficiency of a numerical method with periodic time strides for solving incompressible flows," *Journal of Computational Physics*, 186: 212–229.
28. Bhushan, S., Xing, T., and Stern, F. 2009. "Vortical structures and instability analysis for Athena wetted transom flow with full-scale validation," submitted to *Journal of Fluids Engineering*.
29. Xing, T., Shao, J., and Stern, F. 2007. "BKW-RS-DES of unsteady vortical flow for KVLCC2 at large drift angles," *Proc. of the 9th Intl. Conf. on Numerical Ship Hydrodynamics*, Ann Arbor, Michigan, Aug. 5–8, 187–205.